Is Earth's Surface Insolation Increasing? – Implication for Climate Change Theories

José L. Fernández-Solís * and Bo Young Kim**

Abstract

This paper investigates four critical questions:

First, has the amount of solar irradiance that the Earth receives (Global Horizontal Irradiance) increased over time? This question requires that scientific instruments have recorded, over time, data about solar irradiance. Fortunately, such instruments do exist, and the data has been kept and is available for researchers. The United States National Oceanic and Atmospheric Administration's (NOAA) Surface Radiation budget (SURFRAD) network has seven stations recording the same type of data over time. The data is available and can be analyzed across different spectrums, (NOAA, 2005). Therefore, Earth-ground insolation data from SURFRAD network was analyzed to answer the question. As a result, it was shown that the solar irradiance of the Earth's surface had an increasing trend over the years observed at five out of seven stations in the network and that the amount increased was significant.

Second, what does the upward trend in this data reveal? An upward trend, as found in most stations, indicates a slight increase of solar irradiance at surface level by more than one percent during twenty-five years of observation.

Third, is this trend significant? The Earth facing the sun always receives 410×10^{18} Joules each hour! A one-percent increase means 410×10^{16} Joules per hour! In comparison, the total amount of energy that humans **use in a year** is 410×10^{18} Joules, (Harrington, 2015).

Current theories indicate that global warming due to anthropogenic forcing causes solar radiation to bounce from the different layers of the Earth's atmosphere. If this theory is correct, Earth should be receiving less and not more solar irradiance at ground level, (Brown, Maxwell et al. 2018).

Fourth, what mechanism could allow more solar rays to penetrate all atmospheric layers, plus, increase irradiance? One theory is that the Earth's magnetic shield is weakening allowing the kind of irradiance to reach Earth's surface at increasing levels, as found in this research analysis, (Brooks 2019, and Budyko 1969).

The implications from the data are clear, nothing heats the planet like the sun. There is no anthropogenic mechanism that has the capacity nor the potential, to increase Earth's warming like additional sun rays penetrating Earth's magnetic shield due to its weakening. The cause of the Earth's shield weakening is treated in (Fernández-Solís 2018) research paper that raised the question: "Is there another strand of evidence on the scientific finding that Earth's magnetic field (the B-field) is weakening?"

* José L. Fernández-Solís, PhD – Associate Instructional Professor, Texas A&M University jsolis@tamu.edu
** Bo Young Kim – PhD student, by0705@gmail.com

This paper demonstrates that the solar energy Earth receives from the Sun has been increasing over the years through numerical evidence using the following format:

- Section 1 Introduction
- Section 2 Data and Preprocessing Methods
- Section 3 Adopted Analytical Method and Metrics
- Section 4 Results, Interpretations and Summary of Data
- Section 5 Comments and Conclusion

1. Introduction

Scientists have found that Earth's B-field is weakening. The weakening reason is attributed to an aperiodic Earth's core flip that causes a magnetic pole flip. In other words, where the North Pole is now becomes the South Pole and vice versa. This pole flip has major consequences and implications critical to a normal Earth environment, (Brooks, 2019).

Earth core flip, like the Sun's more periodic flip every 11 years, is a chaotic event where the B-field lines becomes discontinuous and intertwines, it loses density, and becomes chaotic as NASA has proven and shown in (Fernández-Solís, 2018).

When the B-field loses strength, Earth's protection from solar radiation is weakened to the point that it is almost gone. The Sun provides an example of what happens during a magnetic flip (Široký, and Richard 2017). In 2020-2021, the Sun is at a solar minimum where its magnetic field is continuous with hardly any solar flares. Yet SWPC (Space Weather Prediction Center https://www.swpc.noaa.gov/) reports that during this solar minimum observation cycle 25, periodic incidents of dangerous solar radiation reaching the space station and affects satellites in orbit. When an increase of solar radiation is detected whether at a solar maximum or minimum as now in 2021, satellite owners and the space station are warned. At a solar minimum with very few sunspots, the explanation for current warnings could be that Earth's magnetic field has weakened and is no longer shielding these instruments from solar radiation as before, (Livermore et al. 2020).

However, additional strands of evidence that the B-field is weakening are needed. (Vervelidou et al. 2017). Therefore, (Fernández-Solís, 2018) hypothesized that B-field weakening should allow additional Sun insolation to reach Earth's surface when measured over time, the premise of this paper.

The current research found that Earth-ground insolation has been continuously monitored over several decades and at multiple sites-readings that are available to the public, (Smulsky 2020). The data was found, collected, and analyzed to determine if there is a scientific trend on Earth-ground insolation, (Fedorov, and Grebennikov 2017).

Premise

Earth's core flip leads to B-field flip causing B-field weakening allowing Earth-ground insolation increase causing climate change.

According to the US Department of Energy, nothing has the magnitude to affect Earth's climate like the energy coming from the Sun. If the research finds that over time there is an increase in Earth-ground insolation (probably due to B-field weakening), then Earth's climate change rhetoric will need to incorporate a much more significant source of global warming than carbon and other gases, (Harrington, 2015).

2. Data and Processing Methods

The NOAA Surface Radiation budget (SURFRAD) network was established in the mid-nineteen nineties to support climate research with reliable, continuous, long-term measurements of the surface radiation on a national scale (Augustine, et al. 2000; Augustine, et al. 2005; Yang, 2018).

2.1. SURFRAD Dataset

There are a total of seven observatory stations sparsely located in the U.S.: These locations were chosen to represent the diverse and varying climates of the U.S. Observations began in 1995 at the first four stations. The total observations extended to seven gradually by 2003. Daily data continues to be added and can be downloaded on SURFRAD's FTP server.

SURFRAD's dataset includes ground-based irradiances and other meteorological data including air temperature and relative humidity. Data is reported as a 1-minute average (or 3-minute average by 1998). Quality of data is being monitored, and QC (quality control) flags are included in all raw data. Furthermore, calibrations are conducted and reported on SURFRAD's website constantly. The spectral range that SURFRAD's instruments measure include ultraviolet (A, B and C), visible and infrared rays (NOAA 2005). The global horizontal irradiance is calculated using 'direct_n' and 'diffuse' if available, or 'dw_solar' if not. The following are names of instruments and the spectral ranges corresponding to each variable used by SURFRAD from https://gml.noaa.gov/aftp/data/radiation/surfdrad/Bondville_IL/README.:

- 'direct_n': The Normal Incidence Pyrheliometer (NIP).
  The NIP measures direct-normal solar radiation in the broadband spectral range from 280 to 3000 nm. In 2016, it was replaced by the Kipp and Zonen CHP1 pyrheliometer, and it covers the total solar spectrum of solar radiation between 200 to 4000 nm (Augustine and Hodge, 2021).

- 'diffuse': Eppley 8-48 "black and white" pyranometer. (This has been used since 2001.)
  This instrument is sensitive to the broadband spectral range from 280 to 3000 nm.

- 'dw_solar': The Spectrolab SR-75 pyranometer.
  This instrument is sensitive to the broadband spectral range from 280 to 3000 nm.

The SURFRAD's spectrum is the remnant of the solar wind filtered through the different layers of Earth's atmosphere as shown in Figure 1. Under highly weakened conditions ultraviolet (F1) and Xray (D) electrons are likely to reach Earth's surface.

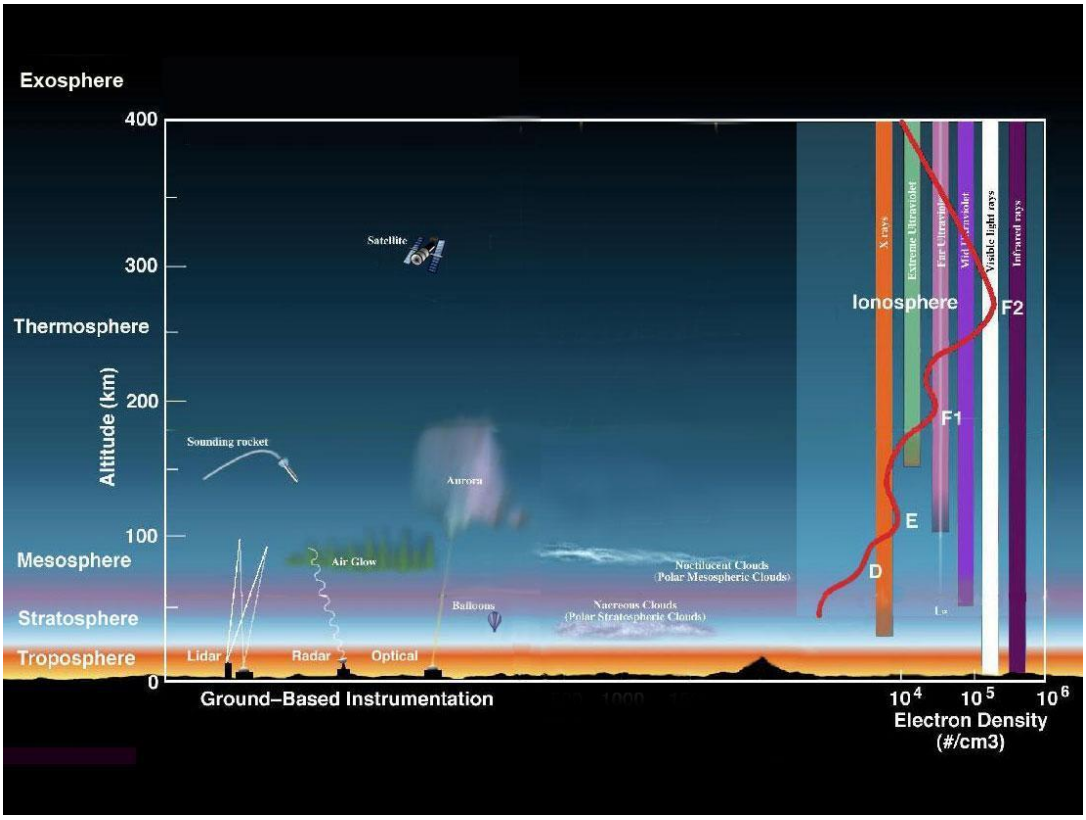

Figure 1. Atmospheric layers and electron densities under Earth's magnetic shield's normal strength (Credit: NASA/Goddard: https://www.nasa.gov/mission_pages/sunearth/science/atmosphere-layers2.html)

Figure 2 is a visual interpretation of the approximate wave range that SURFRAD's instruments measure.

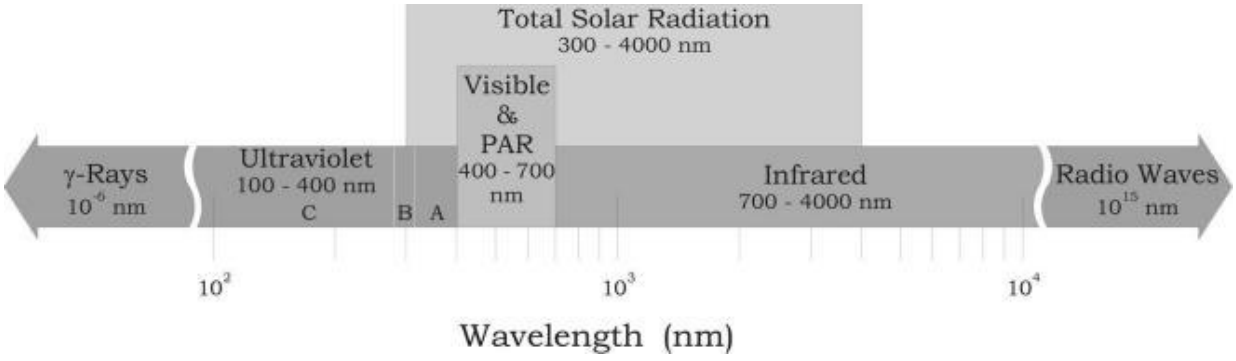

Figure 2. Total Solar radiation wavelengths

2.2. The Sun's Solar Wind, Coronal Mass Ejections and Earth's Atmospheric Layers

The Sun is the origin of visible and invisible light. Invisible light is in the form of a continual outflow of plasma, ionized gas, waves and particles, the solar wind. Earth's atmosphere is protected from direct exposure to the solar wind by its magnetic field which forms a dynamic structure, the Van Allen Belt (discovered in 1958) at the magnetosphere around which the solar wind is diverted. The solar wind plasma carries electrical currents accelerated out of the sun's outer atmosphere at supersonic speeds. Besides the solar wind, the sun also expels intense releases of electromagnetic radiation during cyclic (we are in the 25th observation cycle) solar magnetic flips in what is called Coronal Mass Ejections (CME). CME's are transient, violent events when plasma plus radiation is expelled at speeds more than 1,000 Kilometers per second, and sometimes approaching the speed of light. On top of these two, there is the interplanetary magnetic field (IMF) that changes in density, speed, temperature, strength, and orientation, see Figure 3.

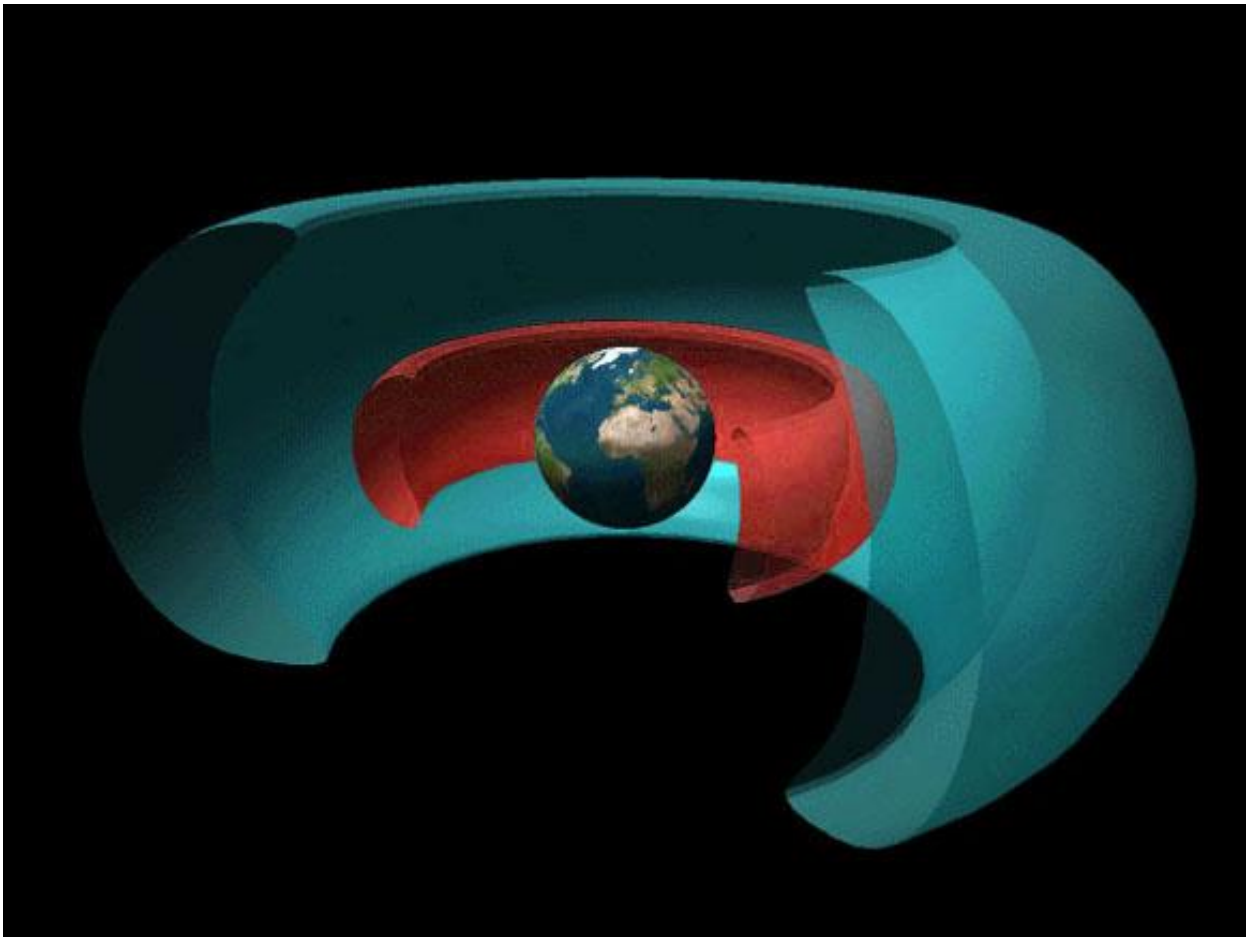

Figure 3. VanAllen radiation belts (Credit JHUAPL, NASA, recolored by cmglee - http://www.nasa.gov/content/goddard/van-allen-probes-reveal-zebra-stripes-in-space)

The solar wind, the CME and IMF encounter first the Earth's atmosphere at the Magnetosphere where the Van Allen Belts buffer some of the electro magnetized plasma

and some radiation rays. Further down towards the Earth, at an altitude of approximately 80 Kilometers, the solar wind hits a population of mix glasses (ozone is one) of the thermosphere crating the ionosphere.

2.3. Area and Period of Interest

The SURFRAD network (Augustine, et al. 2000; Augustine, et al. 2005) is shown in Figure 4. The stations are divided into two groups: Station Group 1 and Station Group 2. The results are explained separately. Stations in group 2 have a shorter time observation period than the ones in group 1.

A small difference in the observation period could affect the results given that the observation periods are not long at all stations; therefore, they are explained separately. The dissimilarity appeared, as evidenced in Section 4. In Figure 4, these are identified as dots of different colors.

For convenience, the station is written as station identification (ID) rather than each station location. Station IDs are in accordance with (Augustine et al. 2000). Station group distinction and station ID are specified in Table 1.

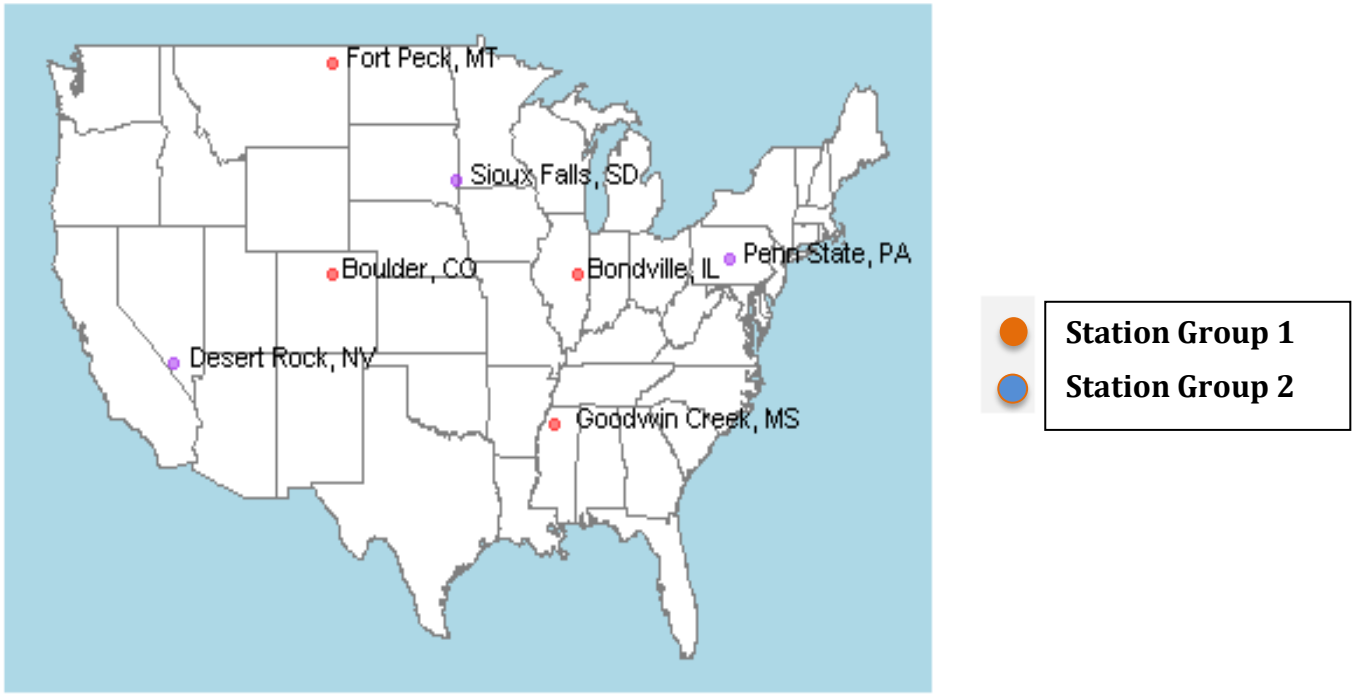

Figure 4. Seven stations in the SURFRAD network.

Table 1. Station information

ID	name	group	start date in raw data	coverage period in this paper
BON	Bondville, IL	1	Jan 1995	Jan 1995 - Dec 2020
FPK	Fort Peck, MT	1	Jan 1995	Jan 1995 - Dec 2020
GWN	Goodwin Creek, MS	1	Jan 1995	Jan 1995 - Dec 2020
TBL	Table Mountain, Boulder, CO	1	June 1995	Jan 1996 - Dec 2020
DRA	Desert Rock, NV	2	Mar 1998	Jan 1999 - Dec 2020
PSU	Penn. State Univ., PA	2	June 1998	Jan 1999 - Dec 2020
SXF	Sioux Falls, SD	2	June 2003	Jan 2004 - Dec 2020

For the stations TBL, DRA, PSU, and SXF in which data is observed from the middle of the first year of observations, we use data from the second year for analysis. The data in the first year at FPK is used, on the other hand, because data began in late January, and the loss of information is relatively small. For each station, the start date of the raw material and the period considered are written in the 4th and the 5th columns of Table 1.

The differences in the analysis results are also examined and interpreted by dividing data into daytime and all-day. The reason for using the daytime data, as well as all-day data, is due to speculation that the average annual solar irradiance, calculated using the all-day data, reflects the values below zero of night-time, and is, therefore, underestimated. If the daytime is defined as the part of a day between sunrise and sunset, it is necessary to define daytime for each station and for each month. A downwelling diffuse solar measurement is used in the raw data to determine when these times are.

2.4. Global Horizontal Irradiance

The question whether insolation (also referred to as solar radiance at ground level) has been increasing over time on Earth's ground can be evidence of the B-field weakening. Therefore, the data will reveal if the average of Earth's horizontal irradiance, the total irradiance from the sun on a horizontal surface on the Earth, has an increasing trend over time. This subsection further describes how to calculate Earth's horizontal irradiance at a certain time from raw data and make it an annual variable called 'annual mean Earth's horizontal irradiance'. This is the variable used for analysis. The abbreviation G are used for convenience.

The best measure of the Earth's horizontal irradiance is the algebraic combination of direct-normal solar ($direct\_n$) and downwelling diffuse solar ($diffuse$), as mentioned in (Augustine et al., 2005; NOAA, 2005) using the following equation:

$$Global\ horizontal\ irradiance = direct\_n \cdot cos(SZA) + diffuse$$

Where the SZA is the solar zenith angle, the global horizontal irradiance can be calculated by two variables: $diffuse$ and $direct$. If the two variables are not of good quality due to

measurement equipment or weather problems, etc., the variable 'downwelling global solar' in files is employed instead.

The preprocessing phase of computing the 'annual-mean-global-horizontal-irradiance' from scratch is explained as follows: First, only observations with 'minute' variables of 0,30 were extracted from the raw data to reduce the size of the data. The daily mean-global-horizontal-irradiances with the values calculated by the above-mentioned method are then obtained. Some can be seen in the form of outliers if the missing or unreliable values are concentrated in the daytime or night-time (or for all-day) in a day. Outliers are the values that are located far away from the trend. Such observations are all considered to be missing values and imputed with a Kalman-smoothing using the 'imputeTS' package (Moritz & Bartz-Beielstein, 2017) in R programming language. Kalman-smoothing was chosen as this (along with na_seadec) yields reasonable results. The 365-day (or 366-day for leap years) averages of daily mean global horizontal irradiance for each year 'Annual (A) mean-global-horizontal-irradiance (G)' were called. This is the variable used for analysis. The abbreviations A and G is used for convenience.

3. Adopted Analytical Method and Metrics

3.1. Simple Linear Regression

To establish the increasing trend of solar insolation on Earth's surface over the years, a simple linear regression model was applied. This method finds a relationship (a straight line) between two continuous variables. It is used to predict dependent variable values by a function of a single independent variable. In this case, 'year' was set on the independent variable and '(A) mean-global-horizontal-irradiance (G)' on the dependent variable with the following relationship:

$$\hat{G} = \beta_0 + \beta_1 \cdot year$$

where $\hat{G}$ is the estimated true mean of G for the population for a given year. An intercept 'β_0' is the average value of G when year is 0. A slope 'β_1' is the expected change in G associated with a 1-unit increase in the value of year. β_0 and β_1 are determined by least square estimation (LSE). The fitted straight line will be shown graphically along with '(A) mean-global-horizontal-irradiance (G)' calculated as described in Section 2.

For each station, each linear regression is fitted for the daytime and all-day data. For this, station index s is defined as $s \in \{BON, FPK, GWN, TBL, DRA, PSU, SXF\}$ and time index t as $t \in \{d, a\}$ to indicate whether the data is daytime (d) or all-day (a). These station indexes and time indexes are written in parenthesis above the abbreviations of our interest. The year index, i, is put on the bottom of them. $n^{(s)}$ indicates the number of years observed in station s. For example, $G_6^{(BON,d)}$ represents the '(A) mean-global-horizontal-irradiance (G)' of the 6-th year (the year 2000 for this station) for the daytime data at station Bondville, IL.

3.2. Evaluation Metrics

Various metrics were used to determine how much solar activity on the Earth's surface has increased (or decreased) over the period. To begin with, the following metrics are based

on the value $\hat{G}$, obtained by simple linear regression. An estimate of annual increasing amounts of G at station s at time t ($AAG^{(s,t)}$) can be defined by the following equation:

$$AAG^{(s,t)}(wm^{-2}/year) = \frac{\hat{G}_{n^{(s)}}^{(s,t)} - \hat{G}_1^{(s,t)}}{n^{(s)}}.$$

This represents how much the amount has increased on average each year. Note that this is equivalent to the slope estimate of simple linear regression analysis.

Instead of the difference between the two values, the increase in proportion is compared. An estimate of increasing rate of G relative to the first year observed at station s at time t($RG^{(s,t)}$) can be defined as follow:

$$RG^{(s,t)}(\%) = \frac{\hat{G}_{n^{(s)}}^{(s,t)} - \hat{G}_1^{(s,t)}}{\hat{G}_1^{(s,t)}} \times 100.$$

However, because all stations have different observed years, scaled values are required about the observation year period. If the irradiance had increased the same rate every year and the amount increased were imposed at the end of each year, the following equation for station s at time t is established:

$$\hat{G}_1^{(s,t)}(1+r)^{(n^{(s)}-1)} = \hat{G}_{n^{(s)}}^{(s,t)}$$

where r is the rate of the yearly increase. Therefore, an estimate of compounding annual increasing rate of G at station s at time t($CARG^{(s,t)}$) can be defined as:

$$CARG^{(s,t)}(\%) = \left\{ \left(\frac{\hat{G}_{n^{(s)}}^{(s,t)}}{\hat{G}_1^{(s,t)}} \right)^{\frac{1}{n^{(s)}-1}} - 1 \right\} \times 100.$$

The results of the statistical significance test regarding AAGs is also analyzed. For each analysis, p-value has to do with 'the annual increasing amount (AAG) and is effective statistically. This is obtained by conducting Student's t-test of the slope of the regression coefficient in a simple linear regression model. The smaller the p-value, the stronger the availability that you should reject the assumption that the slope is 0. That means the estimated coefficient is significant. 'Significance' in tables, shown in section 4, marked as '*' if p-value is less than 0.05, '.' if the value between 0.05 and 0.1, and ' ' if the p-value is greater than 0.1. Usually, if the p-value is less than 0.05, the estimate is considered very significant.

4. Results, Interpretations and Summary of Data

The analysis results by Station Group and time (by all-day and daytime) are closely studied in this section.

4.1. Results at Station Group 1

4.1.1. All-day Data

Figure 7 shows graphs of (G) and prediction values of linear regression $(\hat{G})$ through the years for all-day data of Station Group 1. Each grid represents the stations in Station Group 1. In each graph, the fluctuating blue line stands for G, and the red line is $\hat{G}$. In addition, the bond around the straight line is 95% confidence interval for the mean response.

Solar Cycle 25 is now underway and expected to peak with 115 sunspots in July 2025. Visible light images from NASA's Solar Dynamics Observatory show the Sun at solar minimum in December 2019 (indicated by brackets) and the last solar maximum in April 2014. The previous solar cycle 24 had a maximum in 2014 and a minimum 2009. Hence the data collected, even though cycle 24 shows an increase in (G) is during three solar cycles.

Note: Solar activity, as reported in Figure 5, indicates a decreasing trend (yellow dash line), while our data concludes an increasing trend of solar irradiance at Earth's ground level.

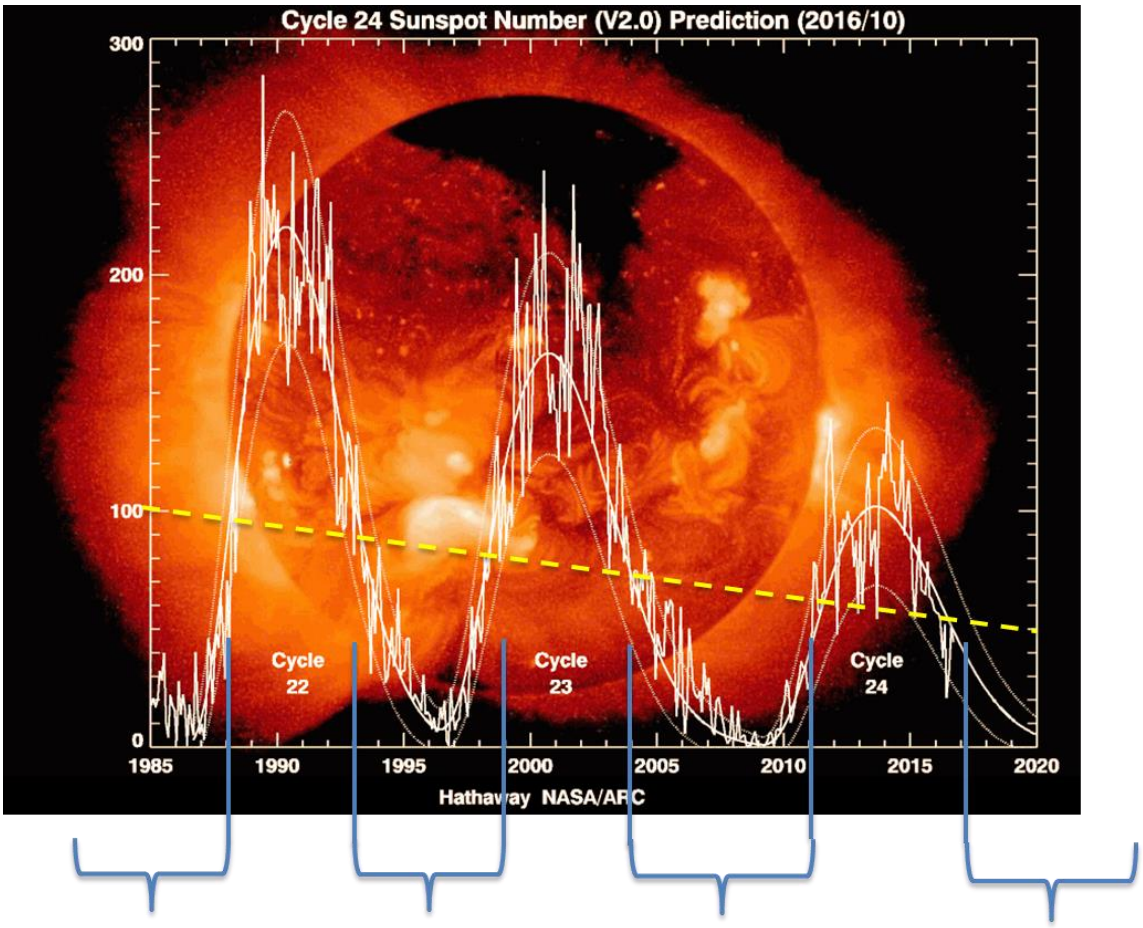

Figure 5. NASA Data during solar cycles 22 to 25. Credit: David Hathaway, NASA, Marshall Space Flight Center - http://solarscience.msfc.nasa.gov/predict.shtml, Public Domain, https://commons.wikimedia.org/w/index.php?curid=28557779

The prediction for Sunspot Cycle 24 as of December 2017 gives a smoothed sunspot number V2.0 maximum of about 101 in late 2013. The smoothed sunspot number V2.0 reached a peak of 116.4 in April 2014. This will probably become the official maximum. This second peak surpassed the level of the first peak (98.3 in March 2012). Many cycles are double-peaked, but this is the first in which the second peak in sunspot number was larger than the first. We are currently over seven years into Cycle 25. The predicted and observed size as of December 2017 makes this the smallest sunspot cycle since Cycle 14, which had a maximum smoothed sunspot number V2.0 of 107.2 in February of 1906.

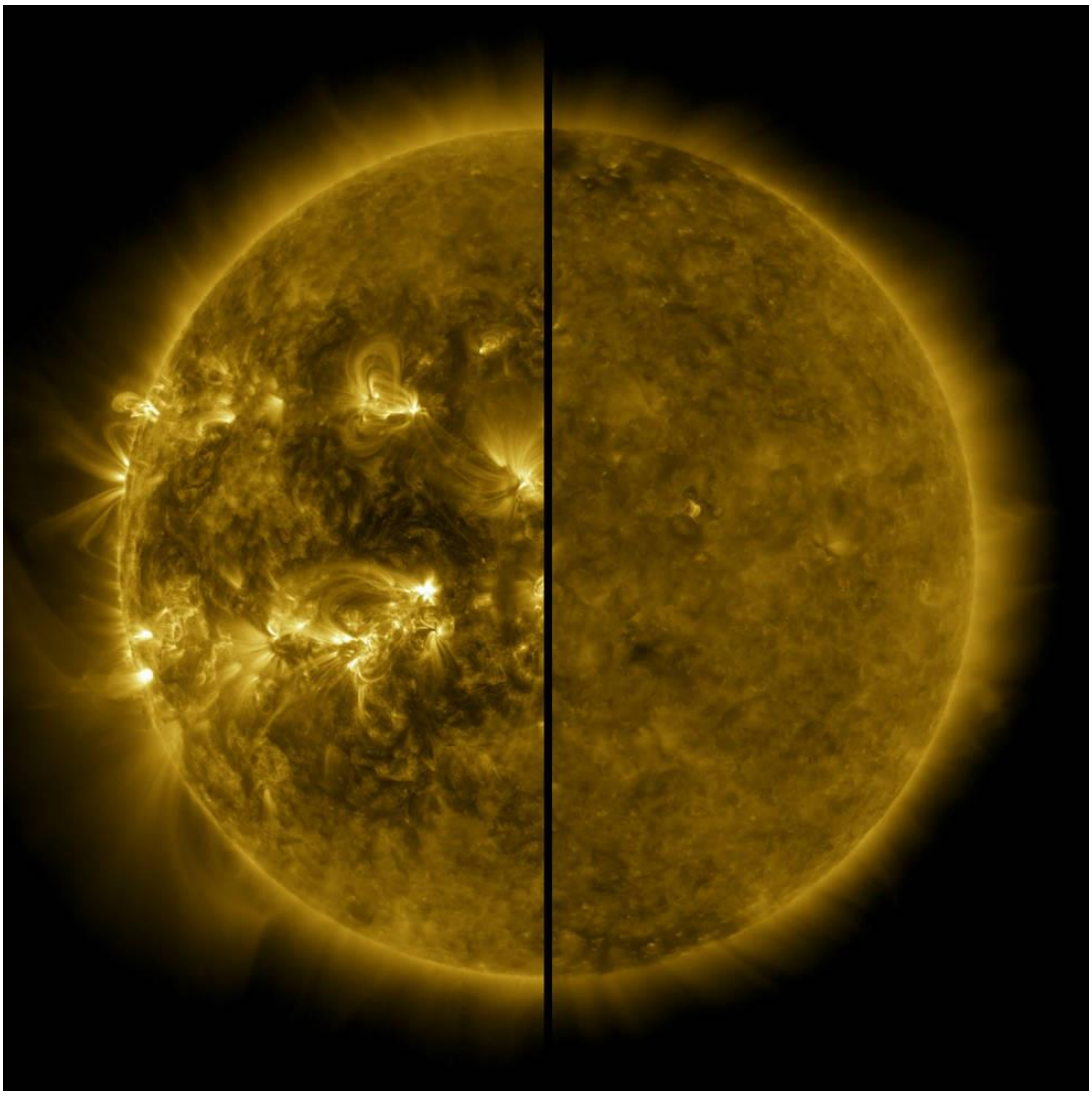

Figure 6. Split image of an active Sun during solar maximum and a quiet Sun during solar minimum. Credits: NASA/SDO

Figure 6 is a split image showing the difference between an active Sun during solar maximum (on the left, captured in April 2014) and a quiet Sun during solar minimum (on the right, captured in December 2019). December 2019 marks the beginning of Solar Cycle 25, and the Sun's activity will once again ramp up until solar maximum, predicted for 2025.

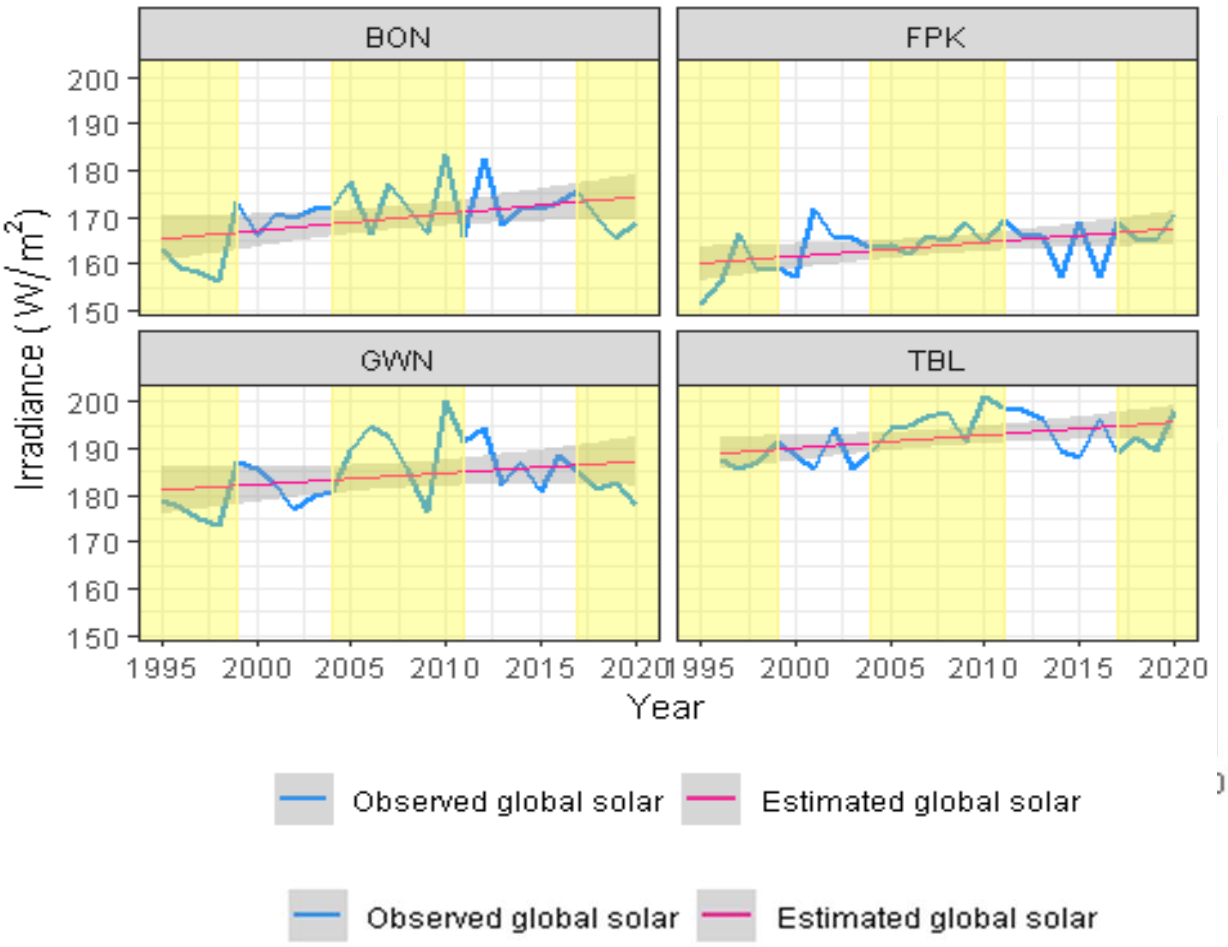

Figure 7. Observed and estimated 'annual-mean-global-solar-irradiance' for all-day data at Station Group 1. (Yellow highlights solar minimum).

Figure 7 shows that for all grids, G is fluctuating, but $\hat{G}$ is upward sloping. Figure 7 trend shows that, in the long run, the all-day average of Global Horizontal Irradiance in Station Group 1 is increasing every year. This can be associated with the numbers in Table 2. The table shows the metrics, and the significance test results for AAG. As observed in Table 2, AAG, RG and $CARG$ are all positive values indicating that solar irradiance on the Earth's surface is on the rise.

Table 2 Evaluation metrics and statistical hypothesis test results for all-day data at Station Group 1

Station ID	AAG	RG	CARG	p-value	significance	period (year)
BON	0.3630	5.4898	0.2140	0.0319	*	26.00
FPK	0.2990	4.6677	0.1826	0.0202	*	26.00
GWN	0.2439	3.3673	0.1326	0.1710		26.00
TBL	0.2782	3.5334	0.1448	0.0314	*	25.00
Average	0.2960	4.2646	0.1685	0.0636	.	25.75

The average for all stations increased by $0.2960 w/m^2$ each year and increased by 0.1685% per year. It increased by 4.2646% over 25.75 years. We mention that there is a difference in measurement characteristics between AAG and RG (or $CARG$). In the ratio calculation, the denominator contains the predicted value of the first year, ($\hat{G}_1$), which is relatively large.

By station, the risen amount and rates are the largest in the BON. (The order of increase of AAG, RG and $CARG$ is consistent for the stations.) It increased by $0.3630 w/m^2$ per year and increased by 0.2140% per year. It increased 5.4898% over 25 years from 1995 to 2020. FPK and TBL follow BON. Meanwhile, GWN has the smallest amount and rates of increase. In addition, the test results of risen amounts were strongly significant for all the other stations. On the other hand, the p-value is 0.1710, and there is insufficient evidence to reject the null hypothesis with β_1 of 0 at GWN. To infer why, you can check that the variation in GWN is large in Figure 7, so the difference between the actual observation G and the straight line is greater than those of the other stations. This means that the standard error is large at GWN. There has also been a recent decline since 2016, which would have made β_1's estimate smaller. These two factors have an adverse effect on proving the significance of β_1.

4.1.2. Daytime Data

Figure 8 is a set of graphs that display G and $\hat{G}$ for the daytime data of four stations in Station Group 1. See Section 4.1.1 above for the explanation of two lines with different colors and the bond.

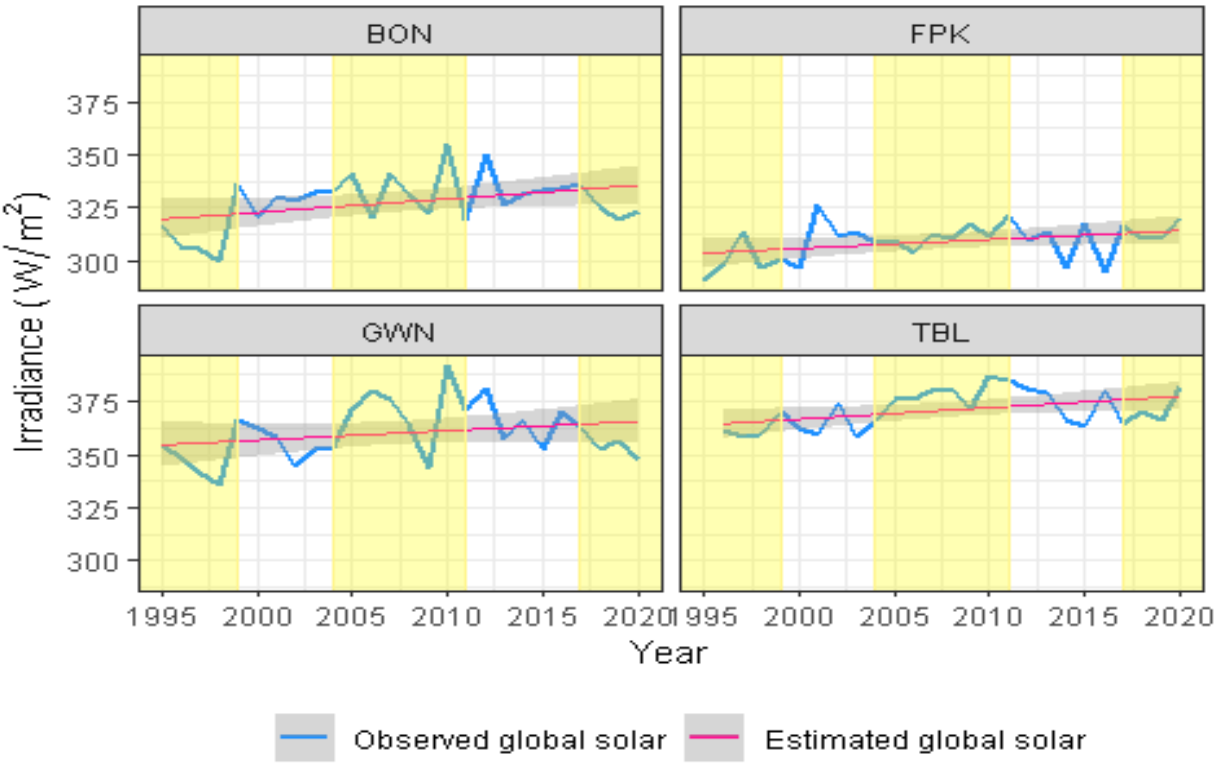

Figure 8. Observed and estimated 'annual-mean-global-solar-irradiance' for daytime data at Station group 1. (Yellow highlights solar minimum)

For the daytime data, $\hat{G}$ is also right-upward and increases throughout the years for all grids. That is, the daytime average-global-horizontal-irradiance has increasing trends. Figure 8, compared to Figure 7, the scales of the y-axis and the exact numbers are different, but line at each station does not seem to differ much from the line in pattern for all-day data. The metrics and statistical hypothesis test values are also shown in Table 3.

Table 3 Evaluation metrics and statistical hypothesis test results for daytime data at Station Group 1

Station ID	AAG	RG	CARG	p-value	significance	period (year)
BON	0.6338	4.9551	0.1936	0.0519	.	26.00
FPK	0.4187	3.4447	0.1356	0.0774	.	26.00
GWN	0.4391	3.0948	0.1220	0.2202		26.00
TBL	0.5422	3.5691	0.1462	0.0297	*	25.00
Average	0.5084	3.7659	0.1494	0.0948	.	25.75

The average for all stations in Table 3 increased by $0.5084 w/m^2$ per year, and by 0.1494% per year. It increased 3.7659% over 25.75 years. When they are compared with the values in Table 2, AAG has been increased by less than twice, but RG and $CARG$ values are not much different than AAG. This is also due to the nature of metrics. The reason that the value of AAG in all-day data is much smaller than in the daytime data is because the value of 0 in the nighttime zone offsets the positive values in the day-time zone when the average G is calculated.

By station, there is the largest increase of the amount and rates in the BON, as with all-day data. It increased by $0.6338 w/m^2$ per year, and by 0.1936% per year. It increased by 4.9551% over 25 years from 1995 to 2020. The TBL follows the BON, followed by FPK and GWN. The risen amount is the smallest in FPK, while the rates are the smallest in GWN. p-value and significance columns prove strong significance in TBL and weak significant results in BON and FPK. On the contrary, in GWN, there is no evidence to reject the null hypothesis, β_1 of zero, with p-value 0.2202. Like the results in all-day data, in this data, the large difference between the actual observation G and the straight line and the small estimate of β_1 would have poorly affected the statistical significance of β_1.

4.2. Results at Station Group 2

4.2.1. All-day Data

Figure 9 is a set of graphs of G and $\hat{G}$ for all-day data for Station Group 2. In DRA, the trend line of $\hat{G}$ has a merely right-upward tendency, even if it just seems flat. In PSU and SXF, they are slightly downwards as years go by. Table 4 lists the relevant metrics and significance test results. The averages on the bottom line indicate that AAG, RG, and $CARG$

are negative. It decreased by $0.1179 w/m^2$ per year, by 0.0758% per year and by 1.2737% for a total of 20.33 years.

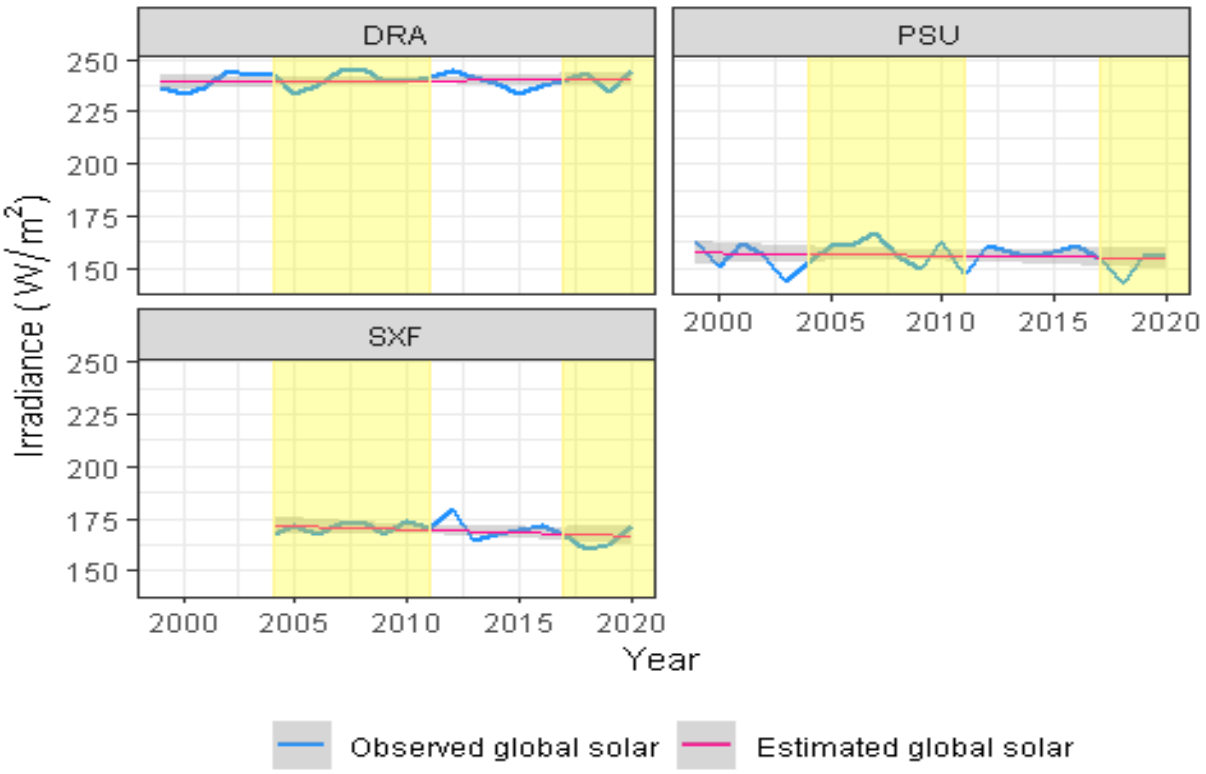

Figure 9. Observed and estimated 'annual-mean-global-solar-irradiance' for all-day data at Station Group 2. (Yellow highlights solar minimum).

Table 4 Evaluation metrics and statistical hypothesis test results for all-day data at Station group 2

Station ID	AAG	RG	CARG	p-value	significance	period (year)
DRA	0.0728	0.63997	0.0304	0.6002		22.00
PSU	-0.1208	-1.61136	-0.0773	0.5740		22.00
SXF	-0.3058	-2.84970	-0.1805	0.1882		17.00
Average	-0.1179	-1.27370	-0.0758	0.4541		20.33

By station, in the DRA, both amount and rates have positive values. It increased by $0.0728 w/m^2$, that is, increased by 0.0304% per year, and by 0.6400% over a total of 22 years. On the other hand, PSU and SXF have negative values. PSU has negative values that are close to zero at either increasing amounts or increasing rates. SXF even has smaller values than that. Solar horizontal irradiance decreased by $0.3058 w/m^2$ and 0.1805% per year at SXF. It decreased by 2.8497% over 17 years. This contrasts with having positive trends for all stations in Station group 1.

The columns of the p-value and significance marks in Table 4, however, the p-values are greater than 0.1 for all stations in Station Group 2. It cannot be concluded that β_1 is different from zero by these numbers. This certainly means that the solar irradiance on the surface neither increased nor decreased statistically at these stations. Then why do these results come out? A valid hypothesis can be that the number of samples (the number of years observed) is relatively small at each station in Station Group 2. The small number of samples can affect the statistical-hypothesis test results.

Figures 7 and 9 provide another possible cause. Observation values of G appear smaller in the late 1990's than in the 2000's. The growth rates from the late 1990's to the early 2000's seem steep. This factor seems to have made the slope larger in Station Group 1. Station Group 2's observations, on the contrary, does not have data from the late 1990's. Hence, the lines' slopes are likely estimated to be small in this group. Therefore, figures in Table 4 should be used with a degree of confidence. In addition to that, analyses should be examined in a longer-term using more data from a statistical point of view.

4.2.2. Daytime Data

Figure 10 represents G and $\hat{G}$ for the daytime data of Station Group 2. The trend of $\hat{G}$ (red line) for each station has a horizontal-like straight line at DRA, and a slightly right-descending straight lines at PSU and SXF. These tend to be like those in Figure 9. The scale of the y-axis is much larger than that of Figure 9 because Figure 10 uses daytime data. Table 5 lists metrics and signification test results for these. The average of all stations in this group decreased by $0.2466 w/m^2$, 0.0856% per year. It also declined 1.4606% over a total of 20.33 years.

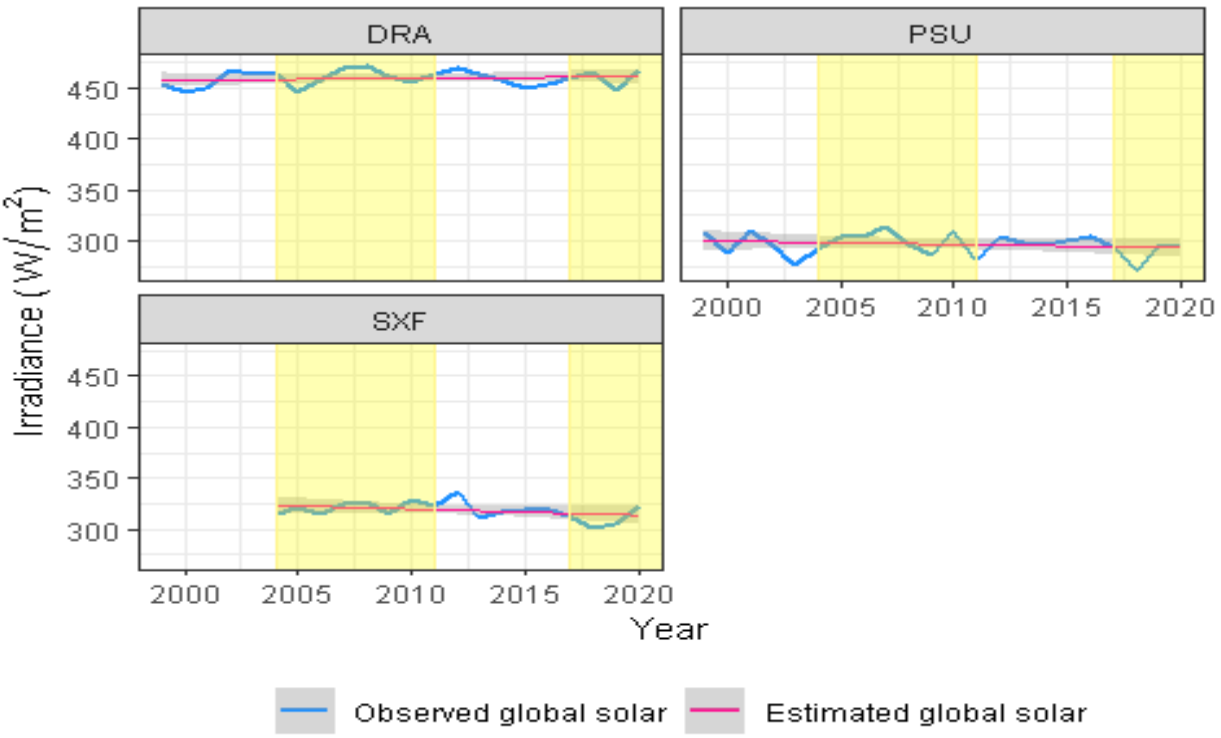

Figure 10. Observed and estimated 'annual-mean-global-solar-irradiance' for daytime data at Station Group 2. (Yellow highlights solar minimum)

Table 5 Evaluation metrics and statistical hypothesis test results for all-day data at Station Group 2

Station ID	AAG	RG	CARG	p-value	significance	period (year)
DRA	0.1806	0.82903	0.0393	0.5205		22.00
PSU	-0.3218	-2.25013	-0.1083	0.4030		22.00
SXF	-0.5986	-2.96068	-0.1877	0.1790		17.00
Average	-0.2466	-1.46059	-0.0856	0.3675		20.33

By station, the DRA has positive values for the increment and rate of increase parameters. It increased by 0.0393%, by $0.1806 w/m^2$ annually, and by 0.8290% throughout 22 years. PSU and SXF have negative values, with SXF having smaller values than PSU. Among them, SXF has had solar irradiance decline by 0.1877%, by $0.5986 w/m^2$ per year, and by 2.9607% over a total of 17 years. Note that the annual increase or decrease amounts are almost double or more different from all-day data in the same group. As mentioned in 4.1.2, this is a feature of the nature of the data. However, it is interesting that they differ more than the all-day and daytime data differences (see Table 2 and 3) in Station group 1. Unlike the amounts, the ratios of all-day and daytime data are not much different.

Nevertheless, there is no reliability of AAG figures in the Daytime data at these stations. This can be seen in the p-values and significance marks in Table 5. P-values are greater than 0.1 for all stations. The same reasons, mentioned in Section 4.2.1, seem to lead to the results that these AAG figures are not significant.

4.3 Summary of Data

Figure 11 is the yearly average solar activity for daytime for Station Group 1 shown in Section 4.1.2. A straight red line is extended to the dotted line of up to 2025. In addition, the area between the red line and the expected solar irradiance of the first year at each station has been shaded.

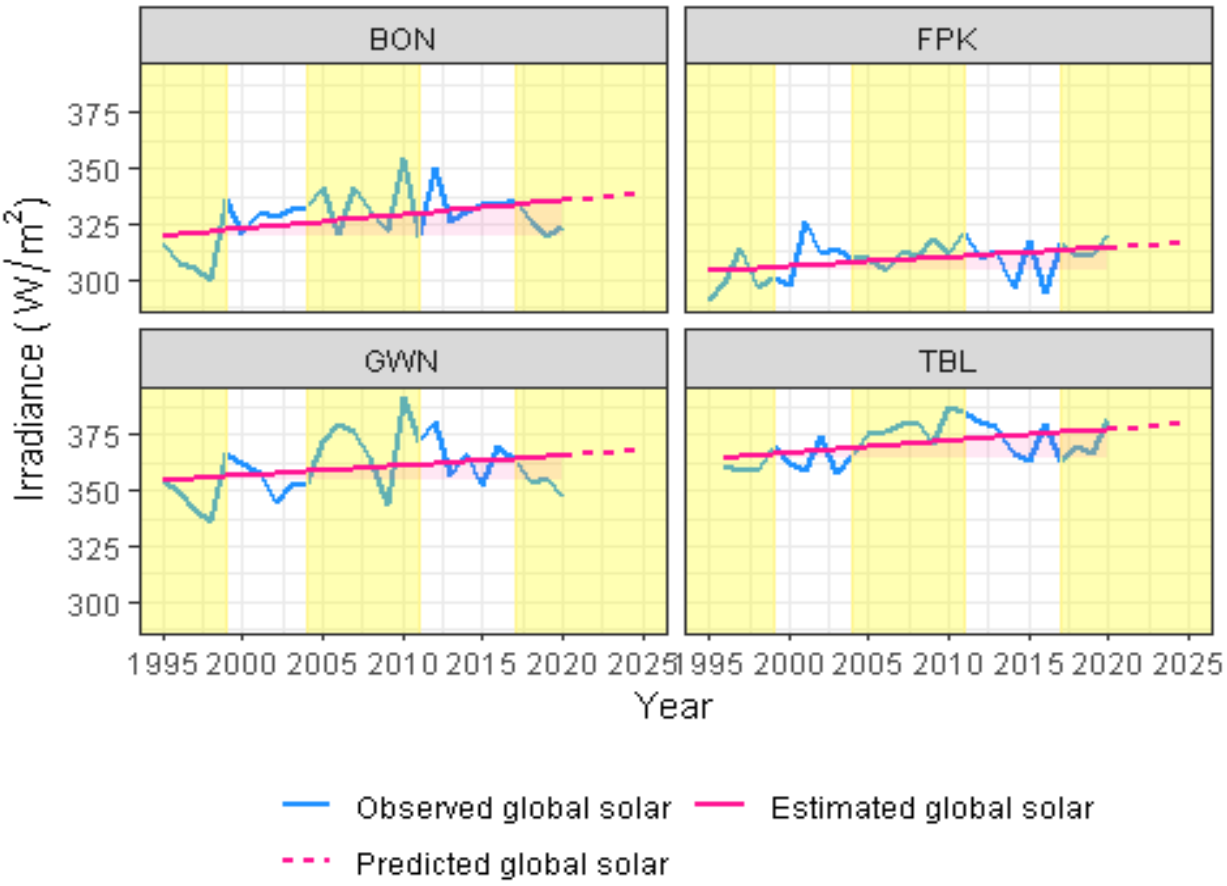

Figure 11. Predicted 'annual-mean-global-solar- irradiance' with observed and estimated values for daytime data at Station Group 1. (Yellow highlights solar minimum).

In the 25 years from 1995 to 2020, the expected global-solar-irradiance at BON increased by $15.8446 W/m^2$. Assuming an annual increase of the same rate, the global solar activity expectation will increase by $19.0135 W/m^2$ from 1995 to 2025. Table 6 is a table of the expected increasing amounts over 30 years, for stations BON, FPK, GWN and TBL.

Table 6. Estimated increasing amount over 30 years at some time in daytime at Station Group 1

Station ID	Estimated increasing W/m^2 amount over 30 years
BON	19.0135
FPK	12.5609
GWN	13.1730
TBL	16.2658
Average	15.2533

How large is the expected change in the intensity of sunlight at $19.0135 W/m^2$ over 30 years in BON? The expected insolation increased will be compared with the amount of electricity produced worldwide in 2008. If this amount of solar energy in Illinois could be converted into electricity, it would be up to 1.2 times the total power output of all power plants in the world. To be specific, total world electricity production was $20{,}261 TWh$ in 2008 (Wikipedia, 2021). This output in watts is $2.31 TW$. Total area in Illinois is $149{,}998 km^2$ and we assume that all points receive the same. It results in $19.0135 W/m^2 \times 10^6 m^2/km^2 \times 149{,}998 km^2 \times 1TW/10^{12} W = 2.8520 TW$.

According to a recent research paper (Augustine and Hodge, 2021), solar insolation on the Earth's surface has decreased since 2012. To refute this claim, Figure 12 is a time series of anomalies obtained from the data we preprocessed and based on their method. Ours includes data for 2020, and there are some minor differences in preprocessing data. Figure 12 confirms that the insolation for 2020 increased again. Furthermore, if linear trend is separately derived for data in 2012 – 2020, as in (Augustine and Hodge, 2021), the slope is gentle and a t-test result of the trend of decreasing is not statistically significant anymore.

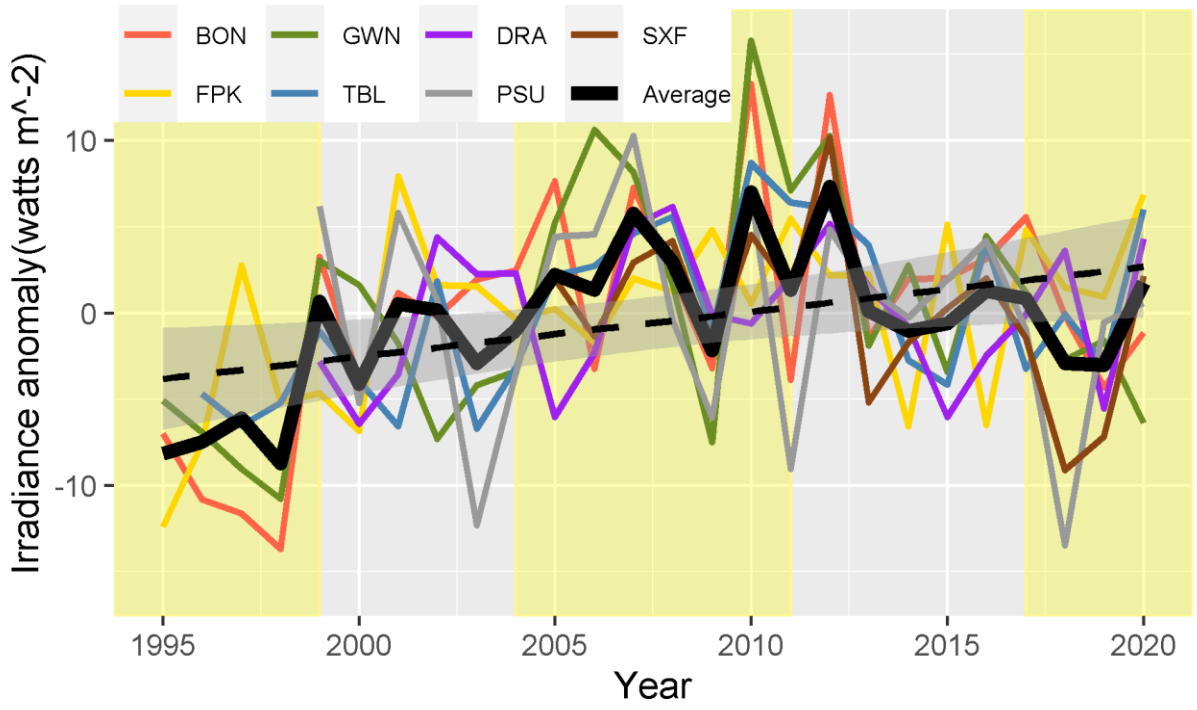

Figure 12. 'annual-mean-global-solar-irradiance' anomalies for the SURFRAD Network. (Yellow highlights solar minimum).

The horizontal zero line in Figure 12 is the overall average of G for all stations for all periods. A thick black line represents the average for each year for all stations. Each colored line is anomaly for each station. A black dashed line is a least-square estimate of the network average value. The bond around the dashed line is 95% confidence interval of the linear fit. Compare it with Figure 2 in (Augustine and Hodge, 2021). (Augustine and Hodge, 2021) separates the above in two parts along year 2012, see Figure 12. The downward trend after 2012 is attributed to some phenomena. Our paper hypothesizes that the phenomena is the solar minimum and therefore, the average value for G should continue and not be segregated.

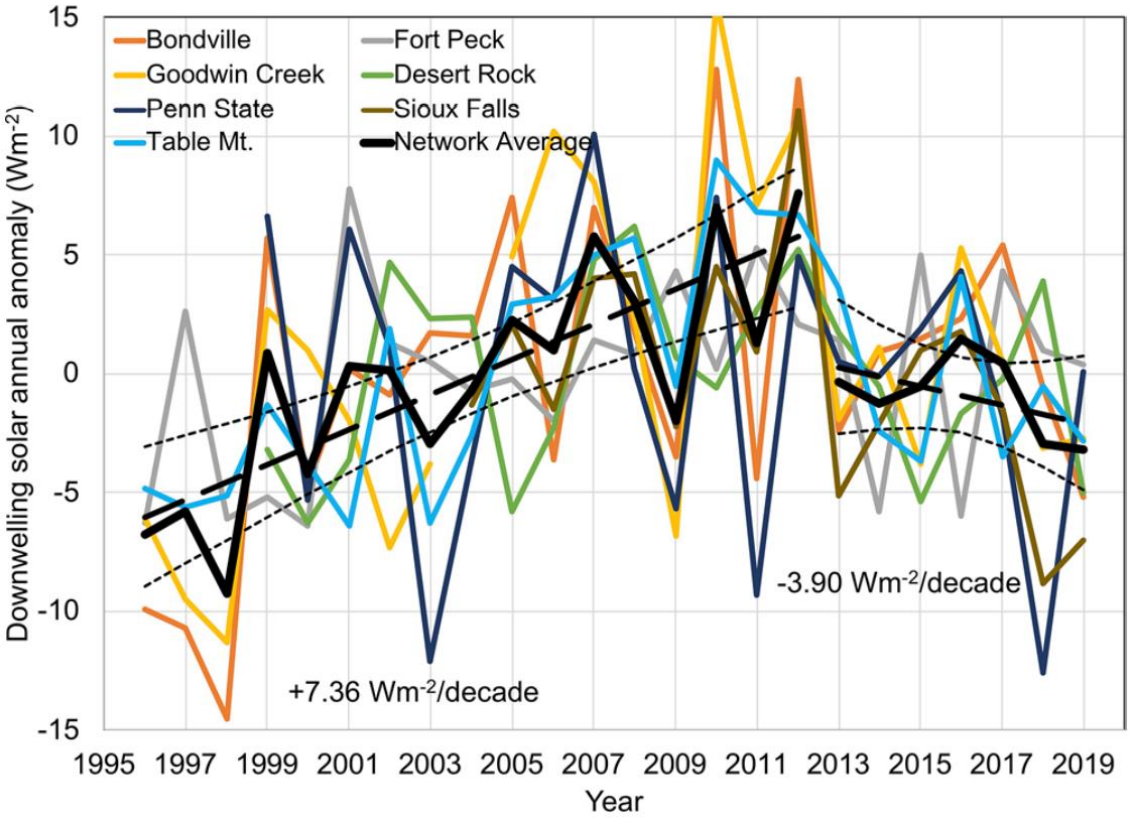

Figure 12. Time series of SW↓ annual anomalies for the SURFRAD Network. The horizontal zero line represents the long-term average over the length of each time series. Network average annual anomalies are denoted by the thick black curve, and color-doced curves are annual anomalies of individual stations. Thick black dashed lines are linear least-squares fits to the network average time series computed separately for 1996-2012 and 2013-2019. Thin black curved dashed lines are 95% confidence intervals o the linear fits. Augustine et al. 2021.

5. Conclusion

Section 4 was analyzed to determine whether the solar irradiance on Earth's surface increases in stations covering various climates in the United States by looking at graphs and numbers. There were increases in several stations: BON, FPK, GWN, TBL, and DRA. The increases were especially dramatic in the late 1990s. Statistical hypothesis tests demonstrated the validity of an increase of solar irradiance in BON, FPK and TBL stations. Assuming an increase of $19.0135 W/m^2$ for 30 years in Illinois, this is 1.2 times the total global production. It can be concluded that the change in solar irradiance is huge, and the increase could be attributed to the weakening of Earth's B-field.

This paper conducts a basic analysis, assuming a simple straight-line relationship between year and solar horizontal irradiance, which means irradiance increases at the same rate over time.

The research raises further questions for research:

1. If the sun activity is decreasing why is the Earth's insolation increasing? More data and more rigorous analysis are needed.

2. If the sun activity is decreasing why are geosynchronous satellites being bombarded with more solar radiation?

3. The magnitude of the Earth's additional insolation needs to be further defined and its consequences honestly analyzed in relation to global warming trends in conjunction and separate from anthropogenic forcing.

4. What are the atmospheric consequences of Earth's magnetic field weakening at all the different layers? Specially, what are the consequences to the Van Allen Belt and the ozone layers?

5. What are the consequences of Earth's magnetic field weakening to Earth's climate?

6. How does Earth's weakening electromagnetic field affects the Van Allen radiation belts?

7. How does weaker Van Allen radiation belts affect Earth's insulation patterns over time?

6. Comments

Our research paper found the data from SURFRAD and analyzed it independently from Augustine et al. 2000, 2005, and 2021. Augustine 2021 paper was of particular interest because of the hypothesis raised regarding the dimming of solar irradiance on a periodic cycle of approximately eleven years. We have a different view to his postulation that irradiance diming can or may be attributed to primarily changes in cloud cover. The cyclic nature is valid in our estimation but from a different perspective, the maximum and minimum solar cycle. This was our initial assessment of the SURFRAD data, and we stand by it. Anthropocentric induced climate change should not pose cycles of variability, however, solar cycles do have the potential to affect climate changes because of the magnitudes of energies involved and their effect on evaporation, cloud formation, rain, and snow precipitation among other weather-related effects. One major observation that we

have raised that lend credence to our postulation is that even though solar cycles appear to be diminishing across the last four solar cycles, the amount of irradiance at surface level has increased. If indeed this can be confirmed by other studies, then the observed evaporation increases can be justified, albeit from the sun and not so much from anthropocentric forcing. We are at the beginning of this type of research, tying the Sun to Earth's climate with more robust data and analysis, and encourage research, debate and critical thinking on cause and effect for a better understanding of the dynamics at work in our world.

References

Augustine, J. A., DeLuisi, J. J., & Long, C. N. SURFRAD–A national surface radiation budget network for atmospheric research. *Bulletin of the American Meteorological Society*, (2000) *81*(10), 2341–2358.

Augustine, J. A., Hodges, G. B., Cornwall, C. R., Michalsky, J. J., & Medina, C. I. An update on SURFRAD—The GCOS surface radiation budget network for the continental United States. *Journal of Atmospheric and Oceanic Technology*, (2005). *22*(10), 1460–1472.

Augustine, J. A., Hodges, G. B., Variability of Surface Radiation Budget Components Over the US From 1996 to 2019—Has Brightening Ceased? *Journal of Geophysical Research: Atmospheres*, *126*(7), (2021). e2020JD033590.

Brooks, Michael. "What's wrong with the north pole?" *New Scientist* 242.3236 (2019): 34-37.

Brown, Maxwell, et al. "Earth's magnetic field is probably not reversing." *Proceedings of the National Academy of Sciences* 115.20 (2018): 5111-5116.

Budyko, Mikhail I. "The effect of solar radiation variations on the climate of the Earth." *tellus* 21.5 (1969): 611-619.

Fedorov, V. M., and P. B. Grebennikov. "Calculation of long-term averages of surface air temperature based on insolation data." *Izvestiya, Atmospheric and Oceanic Physics* 53.8 (2017): 757-768.

Fernández-Solís, J. L. "Relations and Implications of Aperiodic Earth Core/Geomagnetic Field Reversals with Earth Glaciations." (2018). Dr. Solis https://oaktrust.library.tamu.edu/handle/1969.1/169361

Harrington, R. This incredible fact should get you psyched about solar power - US Department of Energy (2015) https://www.businessinsider.com/this-is-the-potential-of-solar-power-2015-9

Livermore, Philip W., Christopher C. Finlay, and Matthew Bayliff. "Recent north magnetic pole acceleration towards Siberia caused by flux lobe elongation." *Nature Geoscience* 13.5 (2020): 387-391.

Moritz, S., & Bartz-Beielstein, T. imputeTS: time series missing value imputation in R. *R J.*, (2017). *9*(1), 207.

National Research Council. “Understanding the Sun and Solar System Plasmas: Future Directions in Solar and Space Physics.” 2005 Washington, D.C.: The National Academies Press. https://doi.org/20.17226/11188.

NOAA Earth System Research Laboratories. ESRL Global Monitoring Laboratory - Global Radiation and Aerosols. (2005, October 1). Retrieved February 9, 2021, from https://www.esrl.noaa.gov/gmd/grad/surfrad/

Široký, Jan, and Richard Linhart. "Solar storm detecting by integrated magnetometer based on anisotropic magnetoresistivity." *2017 25th Telecommunication Forum (TELFOR)*. IEEE, 2017.

Smulsky, Joseph J. "Insolation Periods of Climate Change as a Means of Solving Long-Term Climatic Puzzles." *Modern Environmental Science and Engineering* 6.2 (2020): 190-201.

Vervelidou, Foteini, et al. "On the accuracy of palaeopole estimations from magnetic field measurements." *Geophysical Journal International* 211.3 (2017): 1669-1678.

Wikipedia. Electricity generation. (2021, January 30). Retrieved February 9, 2021, from https://en.wikipedia.org/wiki/Electricity_generation.

Yang, D. Solar Data: An R package for easy access of publicly available solar datasets. *Solar Energy*, (2018). *171*, A3–A12.

Further Reading

Bärenzung, Julien, et al. "Modeling and Predicting the Short-Term Evolution of the Geomagnetic Field." *Journal of Geophysical Research: Solid Earth* 123.6 (2018): 4539-4560.

Cai, Shuhui, et al. "Archaeointensity results spanning the past 6 kiloyears from eastern China and implications for extreme behaviors of the geomagnetic field." *Proceedings of the National Academy of Sciences* 114.1 (2017): 39-44.

Chalk, Thomas B., et al. "Causes of ice age intensification across the Mid-Pleistocene Transition." *Proceedings of the National Academy of Sciences* 114.50 (2017): 13114-13119.

Hasenfratz, Adam P., et al. "The residence time of Southern Ocean surface waters and the 100,000-year ice age cycle." *Science* 363.6431 (2019): 1080-1084.

Kapper, Lisa, et al. "Reconstructing the geomagnetic field in West Africa: first absolute intensity results from Burkina Faso." *Scientific reports* 7.1 (2017): 1-12.

Kozyreva, Olga V., et al. "Ground geomagnetic field and GIC response to March 17, 2015, storm." *Earth, Planets and Space* 70.1 (2018): 1-13.

Laskar, J., F. Joutel, and F. Boudin. "Orbital, precessional, and insolation quantities for the Earth from-20 Myr to+ 10 Myr." *Astronomy and Astrophysics* 270 (1993): 522-533.

Palencia-Ortas, A., et al. "New archaeomagnetic directions from Portugal and evolution of the geomagnetic field in Iberia from Late Bronze Age to Roman Times." *Physics of the Earth and Planetary Interiors* 270 (2017): 183-194.

Panovska, Sanja, M. Korte, and C. G. Constable. "One hundred thousand years of geomagnetic field evolution." *Reviews of Geophysics* 57.4 (2019): 1289-1337.

Panovska, Sanja, C. G. Constable, and Monika Korte. "Extending global continuous geomagnetic field reconstructions on timescales beyond human civilization." *Geochemistry, Geophysics, Geosystems* 19.12 (2018): 4757-4772.

Paluš, M., and D. Novotná. "Northern Hemisphere patterns of phase coherence between solar/geomagnetic activity and NCEP/NCAR and ERA40 near-surface air temperature in period 7–8 years oscillatory modes." *Nonlinear Processes in Geophysics* 18.2 (2011): 251-260.

Stern, Robert J., and Nathan R. Miller. "Neoproterozoic Glaciation—Snowball Earth Hypothesis." *Age (Ma)* 632.1.0 (2019): 632-3.

Tema, Evdokia, Emilio Herrero-Bervera, and Ph Lanos. "Geomagnetic field secular variation in Pacific Ocean: A Bayesian reference curve based on Holocene Hawaiian lava flows." *Earth and Planetary Science Letters* 478 (2017): 58-65.